JACS
JOURNAL OF THE AMERICAN CHEMICAL SOCIETY
pubs.acs.org/JACS
Article

Molecular Design Principles to Elongate the Metal-to-Ligand Charge Transfer Excited-State Lifetimes of Square-Planar Nickel(II) Complexes

Tomohiro Ogawa, Narayan Sinha, Björn Pfund, Alessandro Prescimone, and Oliver S. Wenger*

Cite This: J. Am. Chem. Soc. 2022, 144, 21948−21960
Read Online

ABSTRACT: Square-planar Ni^{II} complexes and their electronically excited states play key roles in cross-coupling catalysis and could offer new opportunities to complement well-known isoelectronic Pt^{II} luminophores. Metal-to-ligand charge transfer (MLCT) excited states and their deactivation pathways are particularly relevant in these contexts. We sought to extend the lifetimes of ^{3}MLCT states in square-planar Ni^{II} complexes by creating coordination environments that seemed particularly well adapted to the $3d^8$ valence electron configuration. Using a rigid tridentate chelate ligand, in which a central cyclometalated phenyl unit is flanked by two coordinating N-heterocyclic carbenes, along with a monodentate isocyanide ligand, a very strong ligand field is created. Bulky substituents at the isocyanide backbone furthermore protect the Ni^{II} center from nucleophilic attack in the axial directions. UV−Vis transient absorption spectroscopies reveal that upon excitation into ^{1}MLCT absorption bands and ultrafast intersystem crossing to the ^{3}MLCT excited state, the latter relaxes onward into a metal-centered triplet state (^{3}MC). A torsional motion of the tridentate ligand and a Ni^{II}-carbon bond elongation facilitate ^{3}MLCT relaxation to the ^{3}MC state. The ^{3}MLCT lifetime gets longer with increasing ligand field strength and improved steric protection, thereby revealing clear design guidelines for square-planar Ni^{II} complexes with enhanced photophysical properties. The longest ^{3}MLCT lifetime reached in solution at room temperature is 48 ps, which is longer by a factor of 5−10 compared to previously investigated square-planar Ni^{II} complexes. Our study contributes to making first-row transition metal complexes with partially filled d-orbitals more amenable to applications in photophysics and photochemistry.

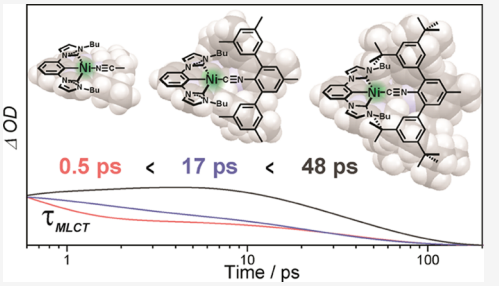

INTRODUCTION

With their more contracted 3d orbitals, first-row transition metals experience inherently weaker ligand fields in coordination complexes than their second- and third-row congeners, and this can negatively affect the photophysical and photochemical performance.[1] One key issue is that weak ligand fields imply energetically low-lying metal-centered (MC) excited states, often associated with substantial molecular distortions, due to electronic transitions between individual d-orbitals with different bonding characters. These distorted MC states offer unwanted nonradiative excited-state relaxation pathways, along which the excitation energy dissipates rapidly and efficiently into molecular vibrations.[2,3]

With its $3d^{10}$ valence electron configuration, Cu^I is not concerned by this fundamental problem,[2,3] simply because no such d−d transitions leading to low-lying MC states exist within the completely filled 3d subshell. Consequently, Cu^I complexes with photoactive metal-to-ligand charge transfer (MLCT) excited states, similar as in precious metal-based coordination compounds, have long been known.[4−9] The very favorable special situation of Cu^I has led to important recent progress in the contexts of lighting,[10−13] solar energy conversion,[14,15] and photocatalysis.[16−18] Aside from $3d^{10}$, the $3d^3$ valence electron configuration as encountered, for example, in Cr^{III} is privileged[19] because the lowest MC states, in this case, can be very weakly distorted owing to the fact that these are so-called spin-flip excited states,[20] in which the bonding situation is largely unchanged with respect to the ground state.[21] Modern coordination chemistry manages to exploit this favorable circumstance, resulting in Cr^{III} complexes with outstanding photoluminescence properties.[22−31]

However, for the $3d^6$ and $3d^8$ valence electron configurations, the presence of low-lying distorted MC states represents a major challenge.[2] In second- and third-row transition metal complexes with the d^6 and d^8 configurations, the respective MC states are often at higher energies than emissive MLCT or other charge-transfer (CT) states,[1,32] making nonradiative relaxation less prevalent and leading to

Received: August 19, 2022
Published: November 23, 2022

https://doi.org/10.1021/jacs.2c08838
J. Am. Chem. Soc. 2022, 144, 21948−21960

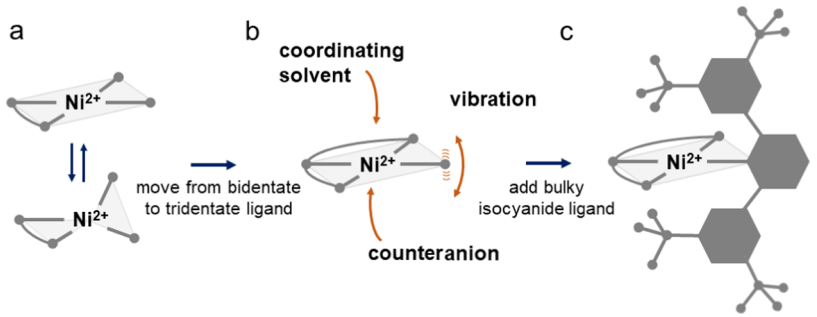

Figure 1. Strategy to enhance the photophysical properties of square-planar Ni^{II} complexes. (a) Typical molecular distortion of Ni^{II} complexes with bidentate and two monodentate ligands, causing unwanted nonradiative excited-state relaxation. (b) Possible excited-state quenching processes in square-planar Ni^{II} complexes, including the nucleophilic attack by solvent or counteranions at the metal center and molecular vibrations in complexes with one tridentate and one monodentate ligand. (c) Improved molecular design used for the elongation of ^{3}MLCT excited-state lifetimes in this study. The coordination environment of Ni^{II} in this scenario, though four-coordinate square-planar, resembles that of an octahedron due to the sterically demanding monodentate ligand shielding the axial coordination positions.

favorable photophysical and photochemical behavior of complexes made from Ru^{II},[33] Ir^{III},[34−37] Pt^{II},[38−49] or Au^{III}.[50,51] Among 3d metals, Fe^{II} has received the most attention concerning the relaxation of MLCT into MC states,[52−67] complemented recently by studies of isoelectronic Co^{III}, Mn^{I}, and Cr^{0} compounds.[68−72] Thus, there is now a substantial body of literature on the photophysics of $3d^6$ compounds, whereas $3d^8$ complexes have remained underexplored in comparison.[2]

Ni^{II} is a prototypical $3d^8$ species and can exist in various coordination environments.[21] $[Ni(OH_2)_6]^{2+}$ is octahedral,[73] but strong-field ligands make four-coordinate square-planar coordination more favorable.[74] Consequently, when aiming at Ni^{II} complexes with elevated MC-state energies due to strong ligand fields, one is automatically confronted with square-planar complexes, in which the absence of axial ligands introduces new challenges. Metal−metal interactions between dz^2 orbitals can lead to aggregation and stacking phenomena, as illustrated by many square-planar Pt^{II} complexes.[43,44,75,76] Recently, a Ni^{II} complex exhibiting weak intermolecular Ni−Ni interactions in dichloromethane solution at room temperature was reported.[77] These interactions seemed to be too weak to provide access to potentially emissive metal−metal-to-ligand charge transfer (MMLCT) excited states. The lack of axial ligands furthermore opens the possibility for nucleophilic attack by solvent or counteranions at the cationic metal center (Figure 1b), thereby creating additional excited-state decay channels not typically present in octahedral coordination compounds. In addition, square-planar d^8 complexes can undergo molecular distortions leading to a symmetry decrease from the D_{4h} to the D_{2d} point group (Figure 1a),[78] and this can facilitate nonradiative excited-state decay. Given these specific challenges, it is perhaps not too surprising that so far, there seem to be no reports of Ni^{II} complexes that luminesce from excited states with direct metal involvement in solution at room temperature. A very recent study reported ligand-based fluorescence from a Ni^{II} complex in solution without direct metal contribution.[79] Weakly luminescent Ni^{II} compounds emitting from triplet states were found in two other recent works, albeit only in the solid state, in which the processes illustrated in Figure 1a/b are largely suppressed.[77,80] Studies in fluid solution at room temperature by transient absorption and transient X-ray absorption spectroscopy were initially limited to porphyrins, phthalocyanines,[81,82] and dithiolato complexes of Ni^{II} and revealed very fast decays to relaxed ^{3}d−d (MC) excited states.[83,84] A recent study aimed to install an emissive (metal-centered) spin-flip excited state but was not successful in that regard.[85] Another recent study claimed that emission is observable for two octahedrally coordinated Ni^{II} complexes in the solid state at 150 K, but the emission was unusually broad and overlapped substantially with the lowest-energy absorption bands.[86] A recent review discussed these results.[20]

More recently, electronically excited states of square-planar Ni^{II} complexes have received increasing attention in the context of photoredox catalysis.[87−97] Many studies have shown that there can be light-free access to Ni-based cross-coupling catalysis,[98,99] whereas others provided evidence for the direct involvement of Ni^{II}-centered triplet excited states via sensitization with Ir^{III} complexes.[92,100,101] This mechanistic debate sparked interest in the electronic excited-state structure and relaxation processes of Ni^{II} complexes in solution. Two recent studies revealed that the series of $[Ni^{II}(dtbbpy)(o\text{-tolyl})X]$ (dtbbpy = 4,4′-di-*tert*-butyl-2,2′-bipyridyl; X = Cl^-, Br^-) complexes exhibits ^{3}MLCT excited states with lifetimes in the range of 5−10 ps.[93,96] The ^{3}MLCT states then relax to ^{3}d−d (^{3}MC) states, in which the complexes adopt a more tetrahedral coordination geometry (resembling the distortion shown in Figure 1a) and which have a lifetime on the order of nanoseconds.[96] To date, these seem to be the compounds with the longest ^{3}MLCT lifetimes (5−10 ps) among Ni^{II} complexes in solution at room temperature. The mechanisms of Ni-catalyzed cross-coupling reactions are still under debate, and recently, the role of charge-transfer (and other) excited states in promoting bond homolysis has been explored.[102−104] Further investigations of the charge-transfer excited-state dynamics of Ni^{II} complexes seem highly desirable to obtain a better understanding of how Ni^{II} complexes operate in photocatalysis.

In this work, we aimed to decelerate nonradiative ^{3}MLCT deactivation to make these charge-transfer excited states more broadly amenable to applications in photophysics and photochemistry. Toward this end, it seemed useful to take some of the lessons learned from prior studies of Pt^{II} compounds into account.[105−110] For instance, to counteract unwanted distortions as illustrated in Figure 1a and to limit the vibrational degrees of freedom, rigid tridentate ligands looked most promising because square-planar Pt^{II} complexes with such chelates often have particularly high photoluminescence quantum yields and long excited-state lifetimes in solution (for example, [Pt(dpyb)Cl] (dpybH = 1,3-di(2-pyridyl)benzene)

https://doi.org/10.1021/jacs.2c08838
J. Am. Chem. Soc. 2022, 144, 21948−21960

Scheme 1. Synthesis and Molecular Structures of the Ligands and Ni^{II} Complexes Investigated Herein

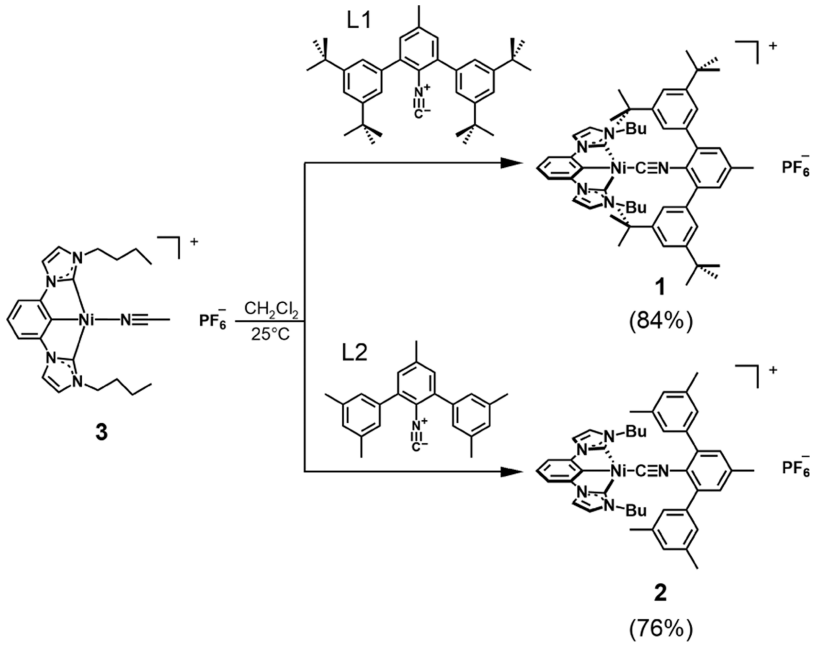

exhibits a photoluminescence quantum yield of 0.60 and τ = 7.2 μs in deaerated CH_2Cl_2 at room temperature).[105] We chose 1,3-bis(3′-butylimidazolyl-1′-yl)benzene (H_3bib, Scheme 1), which should be able to exert a strong ligand field due to its three σ-donating subunits.[80,111,112] To restrict the possibilities for nucleophilic attack by solvent or counteranions as illustrated in Figure 1b, while at the same time maximizing the ligand field strength, the use of a monodentate isocyanide ligand with a *m*-terphenyl backbone looked promising (Figure 1c). Ligands of this type have been used previously to protect different metals in uncommon coordination environments and susceptible oxidation states.[113−117] We hypothesized that in square-planar Ni^{II} complexes, such bulky isocyanide ligands could help to establish axially protected rigid structures with limited degrees of vibrational freedom and shielded axial positions. The monodentate isocyanides were equipped with *tert*-butyl (L1) or methyl (L2)[118] substituents at the *m*-terphenyl side arms (Scheme 1). We synthesized and explored the new complexes [Ni(bib)(Ln)]PF_6 (L1 = **1** and L2 = **2**) along with [Ni(bib)(CH_3CN)]PF_6 (**3**),[80] in an attempt to gain insight into how the photophysical properties and excited-state relaxation of ^{3}MLCT states in Ni^{II} complexes can be controlled by molecular design. Our transient UV−Vis absorption studies indicate that the working hypotheses outlined above are indeed reasonable. The longest ^{3}MLCT lifetime reached in compound **1** is 48 ps, which comes close to the excited-state lifetime of the first emissive Fe^{III} complex reported recently (100 ps),[120,121] suggesting that emission in square-planar Ni^{II} could come within reach.

RESULTS AND DISCUSSION

Synthesis and Characterization. The two bulky monodentate isocyanides were synthesized as described in the Supporting Information (SI). The reaction of the known [Ni(bib)(CH_3CN)]PF_6 precursor complex (**3**)[80] with the isocyanides L1 and L2 in CH_2Cl_2 at room temperature afforded the target Ni^{II} complexes **1** and **2** in good yields (~80%), which were characterized by ^{1}H- and ^{13}C-NMR, elemental analysis, ESI-MS, and single-crystal X-ray crystallography (see SI). Single crystals were grown by liquid−liquid diffusion of *n*-hexane into a CH_2Cl_2 solution of each complex. The X-ray crystal structures of both Ni^{II} complexes have a square-planar geometry (Figure 2 and Table S2). The coordinating structures of the tridentate bib ligands of **1** and **2** are mostly identical to that in the previously reported complex **3**.[80] The Ni−C≡N bond angles ((**1**) 165.5 and (**2**) 173.4°) and C(aryl)−Ni−C(isocyanide) bond angles ((**1**) 160.7 and (**2**)173.4°) deviate substantially from 180°, presumably largely due to crystal packing effects resulting from the need to accommodate the peripheral *tert*-butyl and methyl substituents of L1 and L2 (Figure 2c−d) and partly due to π-back-bonding interactions. In the IR spectra, the C≡N vibrational modes (2131 (**1**) and 2140 (**2**) cm^{-1}) are shifted to a slightly higher frequency ($\Delta\nu$ ~ 15 cm^{-1}) compared to the free ligands L1 and L2 (Figure S7). Previously reported *trans* bis-isocyanide Ni^{II} complexes showed higher C≡N vibrational frequencies (2190−2200 cm^{-1}), and monodentate isocyanides coordinating to azanickelacyclopentenes exhibit C≡N stretching frequencies in the range of 2160−2170 cm^{-1}.[114,122,123] It seems plausible that the lower C≡N vibrational frequencies found in **1** and **2** can be attributed to the trans effect of the aryl carbanion, which has stronger σ−donor and weaker π−acceptor character in comparison to the ligands used in the abovementioned previously reported Ni^{II} isocyanide complexes, leading to the more significant donation of σ electron density from L1 and L2 to Ni^{II} and consequent stronger π back-bonding in **1** and **2**.

The ground-state molecular structures of discrete **1** and **2** were calculated using density functional theory (DFT, see SI page S4 for details) to obtain structural information without the effects of intermolecular interactions found in the X-ray structures. In the obtained DFT-optimized structures, the peripheral *tert*-butyl substituents of L1 shield the axial positions of the metal center well in compound **1**, whereas the methyl substituents of L2 offer at least some partial protection of the Ni^{II} center in compound **2** (Figure S8).

https://doi.org/10.1021/jacs.2c08838
J. Am. Chem. Soc. 2022, 144, 21948−21960

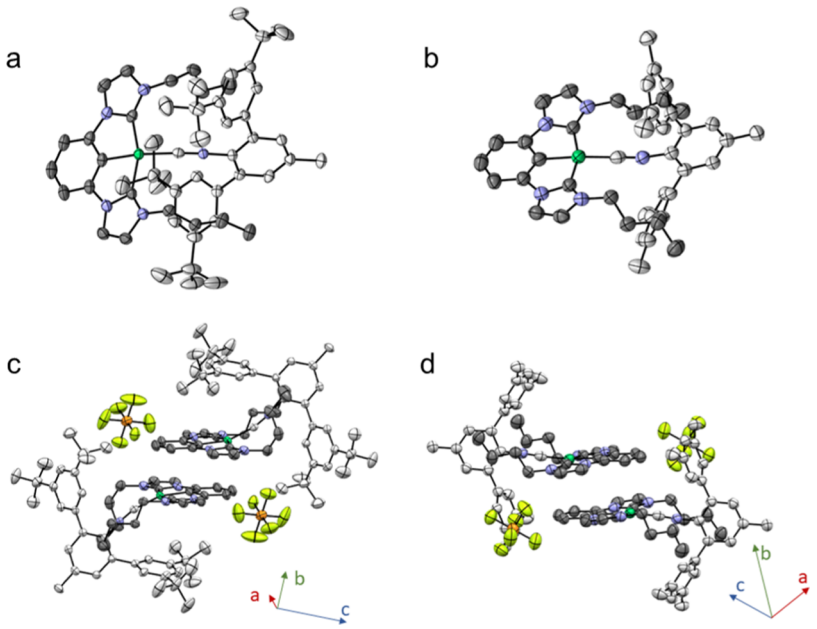

Figure 2. X-ray crystal structures of Ni^{II} complexes (a) **1** and (b) **2** and packing structures of (c) **1** and (d) **2**. Hydrogen atoms are omitted for clarity. 50% probability ellipsoids are shown. Color code: Ni (green), N (blue), C (gray for bib and white for L1 and L2), P (orange), and F (yellow).

Steady-State UV−Vis Absorption Spectroscopy. The UV−Vis spectra of **1**, **2**, and **3** exhibit absorption bands near 400 nm with molar extinction coefficients (ε) on the order of 10^4 M^{-1} cm^{-1} and feature the onset to additional absorption bands at wavelengths shorter than 350 nm (ε > ~10^4 M^{-1} cm^{-1}) (Figure 3a and S9). These latter bands are also present in the free L1 and L2 ligands (dotted traces in Figure 3a) and consequently are attributed to ligand-centered π-π^* transitions, overlapped with other absorptions that emerge in the complexes. Comparing the absorption spectra of **1**, **2**, and **3**, the monodentate isocyanide ligand evidently has a minor influence on the absorption band near 400 nm. This indicates that the respective band involves predominantly the tridentate bib ligand, and the lack of this band in the free ligand spectrum combined with ε values on the order of 10^4 M^{-1} cm^{-1} in the Ni^{II} complexes furthermore suggests that this band is due to MLCT transitions. This hypothesis is confirmed by time-dependent DFT (TD-DFT) calculations focusing on vertical excitations from optimized ground-state structures at the PBE0/6−31G(d,p) level of theory (Figure S11). This specific calculation method was chosen following benchmarking calculations that explored several different methods in earlier studies of related Ni^{II} complexes (Figure S10), which also needed to limit the computation time for comparatively large molecules (see SI page S4 for more details).[77,96,124] Strong transitions were found at around 350−370 nm for all three complexes, at slightly shorter wavelengths than in the experiment (370−440 nm). Natural transition orbital (NTO) analysis for the relevant electronic states (Figure S11) shows that in complexes **1** and **2**, the hole is localized in the metal 3d orbitals, whereas the excited electron is delocalized mainly over the bib ligand framework (~60%) and to some extent over the metal 4p orbital (~20%). Consequently, the lowest absorption bands in Figure 3a are assigned to ^{1}MLCT states, and the transient absorption spectroscopic studies presented below support this assignment. In contrast to complexes **1** and **2**, the S_1 transition orbitals of **3** seem to be similar to those of a Ni^{II} complex that has been previously reported to have an energetically lowest (singlet or triplet) MC state (Figure S11), indicating the strong ligand field imposed by the monodentate isocyanide ligands is essential to shift potentially troublesome d−d (MC) states to higher energies.[124−126] Recent photophysical studies of other Ni^{II} compounds reported absorption bands extending much further into the visible spectral range (500−700 nm),[93,124,127−129] and hence, the Ni^{II} complexes investigated herein have their lowest singlet (charge-transfer) excited states at substantially higher energy. This seems important for establishing longer-lived MLCT excited states.

UV−Vis Transient Absorption Spectroscopy and Identification of Photoactive Excited States. To explore the excited-state evolution and dynamics, UV−Vis transient absorption studies were carried out in CH_3CN and CH_2Cl_2 at room temperature (Figures 3c−d and S15). Initial experiments showed that oxygen from the air has no substantial influence, and hence, aerated samples were used throughout this study. All observable transient absorption spectral changes occur on a timescale shorter than 500 ps. In other words, 0.5 ns after pulsed excitation into the ^{1}MLCT absorption band at 400 nm, all complexes have returned to their electronic ground states. On the very short timescale up to 20 ps (upper half of Figure 3c for **1** in CH_3CN), ground-state bleaching (GSB) of the ^{1}MLCT absorption band is observed between 380 and 440 nm, along with excited-state absorption (ESA) bands detectable between 450 and 520 nm. These ESA bands disappear considerably faster than the GSB, as emphasized by the black downward arrow in the upper half of Figure 3c and the black upward arrow in the lower half of Figure 3c. This observation suggests a two-state scenario, in which an initially populated excited state with a prominent ESA signature decays rapidly to another (energetically lower lying) excited state devoid of any pronounced ESA, and is reminiscent of Fe^{II} polypyridine complexes, in which an initial MLCT excited state (with

https://doi.org/10.1021/jacs.2c08838
J. Am. Chem. Soc. 2022, 144, 21948−21960

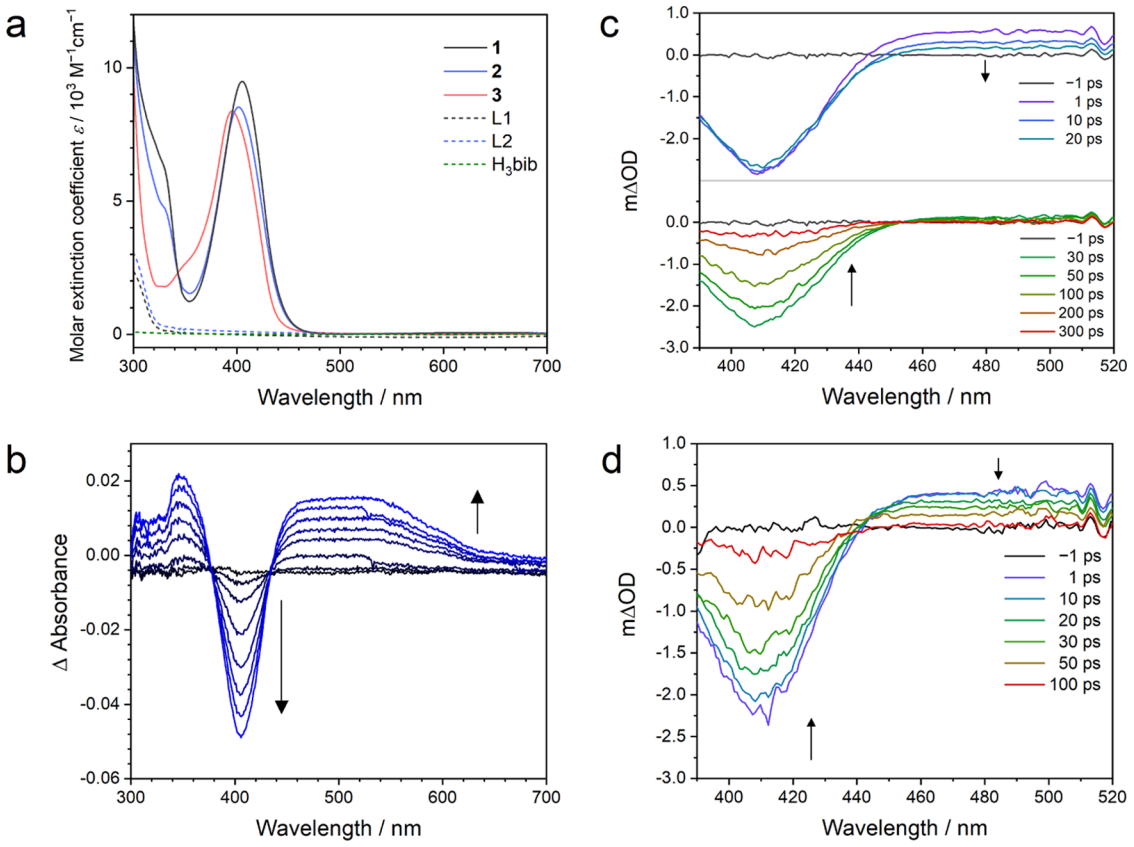

Figure 3. (a) Steady-state UV−Vis absorption spectra of complexes **1**, **2**, **3**, and the free ligands L1, L2, and H_3bib in CH_2Cl_2 at 20 °C. (b) UV−Vis absorption changes of **1** on electrochemical (ligand-centered) reduction at −1.0 V vs Ag/AgCl in deaerated CH_2Cl_2 at 20 °C with 0.1 M $TBAPF_6$ as a supporting electrolyte. The arrows mark the spectral evolution as a function of the time during which the potential was applied. (c) UV−Vis transient absorption spectra of 0.5 mM **1** in aerated CH_3CN at 20 °C, recorded at different delay times as indicated in the insets following excitation at 380 nm. Upper part: Spectra recorded at short delay times, in which changes of excited-state absorption (ESA) are most apparent (arrow pointing downwards). Lower part: spectra recorded at longer delay times, in which changes in ground-state bleaching (GSB) are most apparent (arrow pointing upward). (d) UV−Vis transient absorption spectra of 0.5 mM **1** in aerated CH_2Cl_2 at 20 °C, recorded at different delay times as indicated in the insets following excitation at 380 nm.

prominent ESA bands) decays to $^{3/5}$MC excited states (typically lacking detectable ESA).[119,130]

To identify the nature of the observable ESA bands, (spectro)-electrochemical studies were carried out. The cyclic voltammograms of **1** and **2** exhibit irreversible reduction waves peaking at −0.7 V (vs Ag/AgCl) in CH_2Cl_2 (Figure S12). According to DFT calculations, the LUMO is localized on the π^* orbital of the bib ligand (Figure S13) that is mostly identical to the NTO of the MLCT excited states (Figure S11), similar to the previously investigated analogous Pt^{II} complexes with the same tridentate bib ligand.[110] Thus, the first reduction wave of our Ni^{II} complexes **1** and **2** appears to be ligand centered. Oxidative potential sweeps merely lead to decomposition causing precipitates but do not reveal any clear oxidation waves, in line with a previous study of compound **3**, for which decomposition under oxidizing conditions was also reported.[80] The instability of these Ni complexes upon oxidation limits spectro-electrochemical UV−Vis absorption studies to reductive conditions. When applying a potential of −1.0 V vs Ag/AgCl to a solution of **1** in CH_2Cl_2 containing 0.1 M $TBAPF_6$, the series of UV−Vis absorption difference spectra in Figure 3b can be recorded. Over time, as more and more of the present Ni complexes are reduced, bleaching of the ^{1}MLCT absorption band at 405 nm becomes increasingly pronounced and a new absorption band between 450 and 640 nm emerges (Figures 3b and S14). The latter band is very similar to the ESA feature in the transient absorption spectra (Figures 3c and S15). A similar ESA band has been reported for Os^{II} complexes with structurally closely related tridentate C∧C∧C ligands and bipyridine spectator ligands, in which the lowest MLCT excited states have mixed bipyridine and C∧C∧C ligand character.[131] Thus, it seems plausible to assign the ESA band observable in transient spectroscopy (upper half of Figure 3c, Figure S15) to an MLCT excited state of **1**.[132] The GSB detected on longer timescales (lower half of Figure 3c, Figure S15) are attributed to an electronically excited state for which the spectral ESA characteristics are undetectably weak under these conditions, and this is often the case for MC states.[119,132] Thus, it seems plausible that the initially formed MLCT decays to a lower-lying MC state, in analogy to a recent report of square-planar Ni^{II} complexes, in which a ^{3}MLCT state rapidly decayed to a ^{3}d−d (MC) state.[96] This interpretation implies that the spectra recorded at the earliest delay times in the upper half of Figure 3c already represent ^{3}MLCT spectra, meaning that intersystem crossing from the initially populated ^{1}MLCT state excited at 380 nm to the (relaxed) ^{3}MLCT state takes place on an ultrafast timescale below 1 ps. This is compatible with studies of intersystem crossing kinetics of $3d^6$ metal complexes.[55,119,133−135] In CH_3CN, the ESA bands of **1** decay very rapidly (Figure 3c),

https://doi.org/10.1021/jacs.2c08838
J. Am. Chem. Soc. 2022, 144, 21948−21960

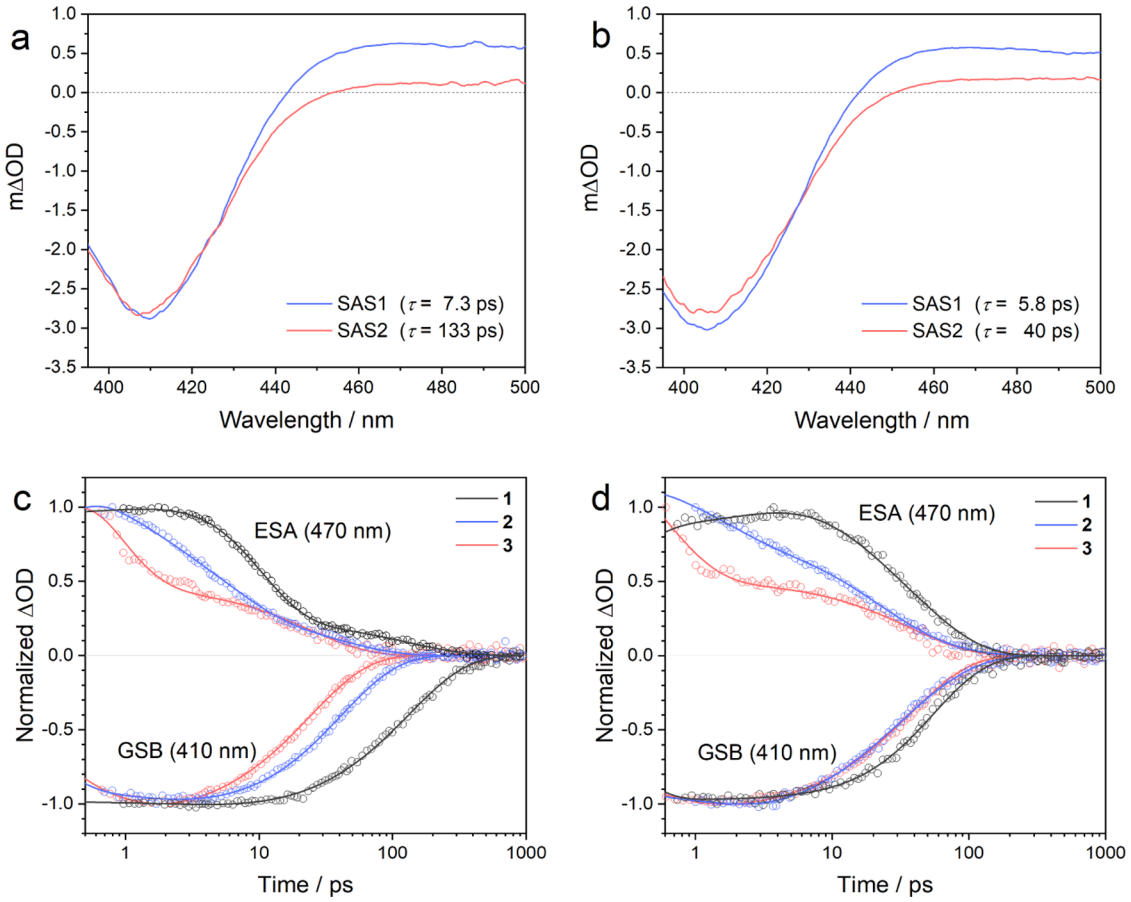

Figure 4. Results from global fittings to the UV−Vis transient absorption spectroscopy data. Species-associated spectra (SAS) of (a) **1** and (b) **2** in CH_3CN at 20 °C following excitation at 380 nm. Decay profiles of the ESA signal at 470 nm and the GSB at 410 nm for **1** (black), **2** (blue), and **3** (red) in CH_3CN (c) and in CH_2Cl_2 (d). The circles represent the experimental data, and the lines represent the fits.

whereas in CH_2Cl_2 the ESA decay becomes slower and occurs with nearly identical kinetics as the GSB recovery (Figure 3d). Evidently, the ^{3}MLCT lifetime of **1** is considerably longer in the noncoordinating CH_2Cl_2 solvent compared to CH_3CN. To further elucidate the ^{3}MLCT decay dynamics and to assess the importance of the isocyanide ligands, the transient absorption data are discussed in more detail in the following section.

Excited-State Dynamics. The experimental UV−Vis transient absorption spectra were analyzed using a global fitting method in the 390 to 500 nm spectral range and the 0.6−1000 ps time domain. The data for compounds **1** and **2** had to be analyzed using a kinetic model involving three consecutive reaction steps (each one of which was associated with a species-associated spectrum (SAS)) to obtain acceptable fits, whereas the data for compound **3** could be adequately fitted with a sequential two-component model (Figure S16). The resulting fitting curves for GSB and ESA kinetics matched the experimental results (Figure 4, Table S4). In general, the individual SAS exhibited distinct ESA (450−550 nm) in their shorter-lived components (SAS0 and SAS1) and negligible ESA in longer-lived components (SAS2), as illustrated in Figure 4a/b and in Figure S17.

In the specific case of compound **1** in CH_3CN (Figure 4a), there is an initial very fast decay process (τ_0 <~3 ps) for which SAS0 (Figure S17) has similar ESA as SAS1 (τ_1 = 7.3 ps, Table 1). We tentatively attribute the initial fast decay (τ_0) to a combination of intersystem crossing and vibrational cooling from the initially excited ^{1}MLCT to the relaxed ^{3}MLCT excited state, which seems in line with the typical timescales for intersystem crossing and following relaxation processes in several Ni^{II} and related first-row metal complexes.[81,83,84,133,136−139] For instance, in a Ni^{II} porphyrin compound, intersystem crossing occurred within 48 fs and vibrational cooling to the relaxed ^{3}d−d state occurred on a timescale of 3.4−26 ps.[81] SAS1 in Figure 4a, associated with a lifetime of 7.3 ps, matches the ^{3}MLCT absorption signature identified in the previous section, whereas SAS2, featuring a lifetime of 133 ps and lacking significant ESA, seems compatible with a ^{3}d−d (MC) state.[96] For compound **2** in CH_3CN (Figure 4b), ^{3}MLCT and ^{3}d−d (MC) lifetimes of 5.8

Table 1. Lifetimes of ^{3}MLCT (τ_1) and ^{3}d−d (MC) Excited States (τ_2) Obtained from Global Fitting[a]

		lifetime (ps) at 20 °C	
compound	solvent	^{3}MLCT (τ_1)	^{3}d-d (τ_2)
1	CH_3CN	7.3	133
2		5.8	40
3		~0.6	24
1	CH_2Cl_2	48	~14
2		17	49
3		~0.5	38

[a]The global fittings of the transient absorption data for compounds **1** and **2** included a third-time component (τ_0) that is tentatively attributed to intersystem crossing and vibrational cooling, see Figures S16 and S17 and Table S4.

https://doi.org/10.1021/jacs.2c08838
J. Am. Chem. Soc. 2022, 144, 21948−21960

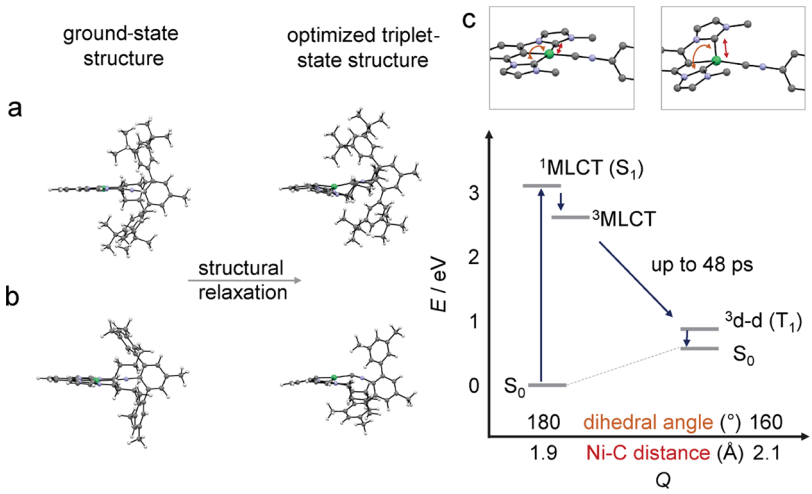

Figure 5. Proposed triplet-state structural relaxation from square-planar (left parts of panels a and b) to approximate tetrahedral coordination geometry (right parts of panels a and b). The initially formed ^{3}MLCT state corresponds to the T_7 state in the square-planar geometry of compounds (a) **1** and (b) **2**. Upon relaxation from T_7 to lower-lying excited states, a structural change from square-planar to distorted tetrahedral occurs. The lowest triplet excited state then corresponds to a metal-centered (^{3}d−d) state both in (a) compound **1** and in (b) compound **2**. (c) Energy-level scheme as a function of key effective nuclear coordinates (Q), involving a torsional motion of the tridentate ligand as illustrated by the orange double arrow in the upper panels. There is a change in C−Ni−C dihedral angle (from ca. 180 to ca. 160°) and a Ni^{II}−carbon (carbene) bond elongation (from ca. 1.9 to ca. 2.1 Å) as marked by the red double arrows in the upper panels of (c).

and 40 ps are extractable from an analogous analysis (Table 1). In the case of compound **3**, the ^{3}MLCT decay kinetics could not be separated from the initial very fast relaxation dynamics (<1 ps, as discussed above) and no accurate ^{3}MLCT lifetime could be determined (Figure 4c), indicating a decay to the ^{3}d−d (MC) state within less than 0.6 ps (Table 1). The ^{3}d−d (MC) excited state exhibits substantially longer lifetimes (133 (**1**), 40 (**2**), and 24 (**3**) ps in CH_3CN) than the ^{3}MLCT state.

Focusing back on the ^{3}MLCT excited-state lifetime, we note that in noncoordinating CH_2Cl_2 that lifetime is elongated in compounds **1** and **2** compared to CH_3CN (Figure 4d). The record lifetime is 48 ps for compound **1** with the bulkiest monodentate isocyanide ligand in CH_2Cl_2 (Table 1). Thus, the data in Table 1 reveal a clear trend: The ^{3}MLCT lifetime increases along the compound series **3** < **2** < **1** and furthermore increases when going from CH_3CN to CH_2Cl_2. The solvent trend could reflect both differences in polarity and in coordinating nature, whereas the compound trend is in line with increasing ligand field strength (lifetime elongation from **3** to **2**) and with increasing steric protection of the Ni center by the monodentate isocyanide ligand (further lifetime elongation from **2** to **1**).

Triplet Excited-State Characteristics. The triplet-state characteristics were further studied computationally. To determine the triplet energies in the Franck−Condon region, triplet-state TD-DFT calculations were carried out, at first using ground-state optimized structures (left part of Figure 5a/b, Tables S10−S12). The ^{3}MLCT states in the Franck−Condon region were found at roughly 3.1 eV (T_6 and T_7 in Tables S10 and S11; Figure S21), where these two states are energetically close to each other. The NTO and energies of T_7 were used as a representative ^{3}MLCT state due to its clear MLCT character. The lowest triplet states are mostly MC states (T_1−T_3) even in square-planar geometry. In Pt^{II} complexes with the same tridentate bib ligand, the lowest triplet states were assigned to ligand-centered (LC) states and had an energy of approximately 2.9 eV.[110] In our Ni^{II} complexes, the equivalent ^{3}LC states correspond to the T_4 excited states, featuring a similar energy as in the previously investigated Pt^{II} compounds (~2.7 eV). Evidently, in the Ni^{II} complexes explored here, there are energetically lower-lying ^{3}MC states, representing a key difference to Pt^{II} photophysics, in line with expectation.

In the initially formed ^{3}MLCT states, the change to a formal Ni^{III} oxidation state with a d^7 electron configuration can potentially entail a structural reorganization, leading to a distortion away from square-planar coordination (Figure 1a). Consequently, the optimized *triplet* states were calculated to obtain relaxed triplet energies and structural characteristics (a different functional was used for triplet-state optimization, see SI page S4 for details, Tables S13−S15, Figures S18 and S19). The resulting optimized relaxed triplet structures are shown on the right-hand sides of Figure 5a/b. Although the ligand backbones are not significantly distorted, the primary coordination sphere around the Ni center undergoes substantial reorganization. Specifically, the two *N*-heterocyclic carbene (NHC) subunits of the tridentate ligand become tilted with respect to each other, manifesting in a torsion angle decreasing from close to 180° to near 160° (orange double arrows in the upper panels of Figure 5c). Furthermore, the average distance between the metal centers to the two respective coordinating NHC−carbon atoms becomes ~0.2 Å longer (red double arrows in the upper panels of Figure 5c). Full structural details are given in Table S5 of the SI. This structural distortion stabilizes the lowest triplet state by ~2.0 eV with respect to the ^{3}MLCT state in square-planar geometry, as illustrated by the energy-level scheme in Figure 5c, while simultaneously destabilizing the S_0 state by ~0.8 eV (Table S6 and Figure S19). The resulting lowest triplet states in these relaxed geometries were consistently found at an energy close to 0.2 eV above the S_0 state for the tetrahedrally distorted complexes **1** and **2** (Table S6 and Figure S19). The natural transition orbital analysis for the relaxed T_1 states of compounds **1**−3 reveals that the hole is localized on the d_z^2 orbital (~97%) and the excited electron is mainly localized on the $d_{x^2-y^2}$ orbital (metal contribution = ~52%) with a

https://doi.org/10.1021/jacs.2c08838
J. Am. Chem. Soc. 2022, 144, 21948−21960

significant ligand contribution (~40%) (Figure S20). Consequently, this relaxed T_1 state of the tetrahedrally distorted complexes seems indeed assignable to a ^{3}d−d state, in line with a recent study of square-planar Ni^{II} complexes.[96] The orbital contributions of the pertinent natural transition orbitals (Figure S20) indicate that the electron density at the tridentate bib ligand is substantially higher in the ^{3}MLCT (T_2) state (53−63%, Figure S20) relative to the ^{3}d−d (T_1) state (34−43%), which is in line with the expectable changes upon internal conversion from a ^{3}MLCT to a ^{3}d−d state.

The overall excited-state evolution emerging from the combined experimental and computational studies is summarized in Figure 5c. Following excitation into ^{1}MLCT excited states, intersystem crossing into the lowest ^{3}MLCT states occurs on a timescale below 0.6 ps; ^{3}LC states as commonly observed in Pt^{II} complexes do not play an appreciable role.[110] In the ^{3}MLCT excited states, the nickel complexes likely maintain the approximate square-planar geometry of the electronic ground state (S_0), but upon further relaxation to the ^{3}d−d (T_1) excited state, the primary coordination sphere reorganizes such as to adopt an overall geometry closer to tetrahedral.

Interestingly, there seem to be substantial differences concerning the structural rearrangement of compounds **1** and **2** in Figure 5a/b, which can be traced back to the different levels of steric hindrance provided by L1 and L2. Specifically, the Ni−C≡N bond angle in **1** remains essentially unaffected by the structural relaxation from square-planar toward tetrahedral geometry (174.7−175.5°), whereas in **2** the respective bond angle decreases from 173.4 to 156.2°, according to the DFT calculations. This finding suggests that the *tert*-butyl substituents of L1 are able to restrict the (unwanted) structural rearrangement much better than the methyl substituents of L2. Consequently, it seems adequate to conclude that bulky substituents placed in the axial position of square-planar Ni^{II} complexes can play an important role in extending the lifetime of ^{3}MLCT excited states because these substituents can help prevent the structural distortion leading to relaxed lower-lying ^{3}d−d excited states.

The longest ^{3}MLCT lifetime reached was 48 ps (Table 1), which is roughly half the lifetime reported recently for the first emissive excited state of a Fe^{III} compound (100 fs).[121] Against this background, it seemed reasonable to search for photoluminescence from the ^{3}MLCT excited states of **1** in deaerated CH_2Cl_2 solution at 20 °C and in a 2-MeTHF glass matrix at 77 K, but our attempts were unsuccessful and did not provide reproducible emission spectra nor excitation spectra that would match the UV−Vis absorption spectra in Figure 3. Thus, it seems that the ^{3}MLCT states of our Ni^{II} complexes are either completely nonemissive or luminesce with quantum yields that are below our instrument's sensitivity. Assuming that the radiative rate constant (k_r) for ^{3}MLCT to S_0 relaxation of Ni^{II} complexes are on the same order of magnitude as in related Pt^{II} complexes (10^4−10^5 s^{-1}),[140−143] a 50 ps ^{3}MLCT lifetime would imply a luminescence quantum yield (ϕ) on the order of 10^{-6}−10^{-7} (based on the relationship $\phi = k_r \times \tau$). This is a factor of 10−100 below the detection limit of common luminescence spectrometers, and to reach that limit, a further ^{3}MLCT lifetime elongation to 500 ps−5 ns would seem necessary. A key difference between our Ni^{II} compounds and the previously reported Fe^{III} complex with a luminescent LMCT state featuring a lifetime of only 100 ps is the fact that the emission transition in the iron(III) complex was spin-allowed,[121] whereas in our cases it would be formally spin-forbidden, resulting in an inherently lower radiative rate constant. The 48 ps lifetime is too short to allow for diffusion-controlled bimolecular reactions but could be sufficiently long for photoredox catalytic reactions in pre-aggregated encounters between the Ni^{II} complex and substrate molecules, in analogy to what appears to be the likely reaction mode of similarly short-lived (doublet) excited states of organic radical anions.[144−149]

CONCLUSIONS

Our study demonstrates that the lifetimes of ^{3}MLCT excited states of square-planar Ni^{II} complexes follow clear molecular design principles. Specifically, our work reveals the importance of the following structural aspects: (i) a strong ligand field as a result of σ-donation and π-back-bonding, (ii) rigidity and steric hindrance to counteract geometrical distortion in electronically excited (triplet) states, and (iii) protection of the metal center from the chemical environment, in particular from nucleophilic attack along axial directions. The observable trends in ^{3}MLCT lifetimes along the series of compounds **3** < **2** < **1** (0.5 ps, 17 ps, 48 ps in aerated CH_2Cl_2 at 20 °C, Table 1) along with the results in Figure 5 provide the key basis for this conclusion.

^{3}MLCT relaxation occurs nonradiatively to a lower-lying ^{3}d−d (^{3}MC) excited state, in which the primary coordination sphere undergoes distortion from square-planar toward more tetrahedral geometry, as reported previously for other four-coordinate Ni^{II} complexes.[93,96] However, the tridentate nature of the coordinated H_3bib ligand limits the level of distortion when compared to previously studied Ni^{II} complexes with bidentate chelate ligands.[96] Rigidification of the tridentate chelate ligand might therefore represent an attractive way to counteract this unwanted distortion even further to decelerate the internal conversion from the ^{3}MLCT to the ^{3}MC state, such as to obtain even longer-lived (and potentially emissive) ^{3}MLCT states. Further improvements of the steric protection in axial directions seem possible with suitably designed monodentate ancillary ligands, and this could help maintain a square-planar coordination environment throughout the entire excited-state evolution pathway. In other words, gaining control over the second coordination sphere could become a particularly important aspect of the photophysics of 3d^8 metal complexes. The influence of the second coordination sphere currently seems to be yet an underappreciated aspect in the design of new photoactive coordination compounds, at least among first-row transition metal complexes.[150−153] The different extents of excited-state distortions permitted by L1 and L2 due to their different steric demand and the ensuing sizeable differences in ^{3}MLCT lifetimes in compounds **1** (17 ps) and **2** (48 ps) illustrate the potential of this "axial protection" design strategy. This is particularly true in comparison to **3** (0.5 ps) and many previously investigated square-planar Ni^{II} complexes, in which this effect is absent.

Compared to octahedral complexes with the 3d^6 valence electron configuration, square-planar 3d^8 complexes have received less attention until now from the photophysics community, and we hope the insights gained herein will help make square-planar Ni^{II} complexes more amenable to applications in photophysics and photochemistry. In the bigger picture, our study complements recent work on charge transfer excited states in first-row transition metal complexes

https://doi.org/10.1021/jacs.2c08838
J. Am. Chem. Soc. 2022, 144, 21948−21960

and contributes to elucidating the convoluted excited-state relaxation processes in this emerging class of compounds.

■ ASSOCIATED CONTENT

Supporting Information

The Supporting Information is available free of charge at https://pubs.acs.org/doi/10.1021/jacs.2c08838.

General procedures and equipment details; synthesis and characterization of ligands and metal complexes; X-ray crystallographic data; cyclic voltammograms; spectro-electrochemistry data, spectroscopic data, and DFT and TD-DFT data (PDF)

Accession Codes

CCDC 2177351−2177352 contain the supplementary crystallographic data for this paper. These data can be obtained free of charge via www.ccdc.cam.ac.uk/data_request/cif, or by emailing data_request@ccdc.cam.ac.uk, or by contacting The Cambridge Crystallographic Data Centre, 12 Union Road, Cambridge CB2 1EZ, UK; fax: +44 1223 336033.

■ AUTHOR INFORMATION

Corresponding Author

Oliver S. Wenger − *Department of Chemistry, University of Basel, 4056 Basel, Switzerland;* orcid.org/0000-0002-0739-0553; Email: oliver.wenger@unibas.ch

Authors

Tomohiro Ogawa − *Department of Chemistry, University of Basel, 4056 Basel, Switzerland;* orcid.org/0000-0001-7298-0149

Narayan Sinha − *Department of Chemistry, University of Basel, 4056 Basel, Switzerland*

Björn Pfund − *Department of Chemistry, University of Basel, 4056 Basel, Switzerland;* orcid.org/0000-0003-0936-2975

Alessandro Prescimone − *Department of Chemistry, University of Basel, 4058 Basel, Switzerland;* orcid.org/0000-0002-3631-5210

Complete contact information is available at: https://pubs.acs.org/10.1021/jacs.2c08838

Notes

The authors declare no competing financial interest.

■ ACKNOWLEDGMENTS

Funding from the Swiss National Science Foundation through grant number 200020_207329 is acknowledged. T.O. acknowledges the Japan Society for the Promotion of Science (JSPS) for an Overseas Research Fellowship (application number 202160473) and a Swiss Government Excellence Scholarship for Foreign Scholars and Artists (ESKAS number 2020.0027). B.P. acknowledges a Ph.D. grant (number 14583224) by the National Research Fund, Luxembourg.

■ REFERENCES

(1) McCusker, J. K. Electronic structure in the transition metal block and its implications for light harvesting. *Science* **2019**, *363*, 484−488.

(2) Wegeberg, C.; Wenger, O. S. Luminescent First-Row Transition Metal Complexes. *JACS Au* **2021**, *1*, 1860−1876.

(3) Förster, C.; Heinze, K. Photophysics and photochemistry with Earth-abundant metals − fundamentals and concepts. *Chem. Soc. Rev.* **2020**, *49*, 1057−1070.

(4) Dietrich-Buchecker, C. O.; Marnot, P. A.; Sauvage, J. P.; Kirchhoff, J. R.; McMillin, D. R. Bis(2,9-Diphenyl-1,10-phenanthroline)copper(I) - A Copper Complex With a Long-Lived Charge Transfer Excited State. *J. Chem. Soc., Chem. Commun.* **1983**, 513−515.

(5) Cuttell, D. G.; Kuang, S. M.; Fanwick, P. E.; McMillin, D. R.; Walton, R. A. Simple Cu(I) Complexes with Unprecedented Excited-State Lifetimes. *J. Am. Chem. Soc.* **2002**, *124*, 6−7.

(6) Lazorski, M. S.; Castellano, F. N. Advances in the Light Conversion Properties of Cu(I)-Based Photosensitizers. *Polyhedron* **2014**, *82*, 57−70.

(7) Armaroli, N. Photoactive Mono- and Polynuclear Cu^{I}-Phenanthrolines. A Viable Alternative to Ru^{II}-Polypyridines? *Chem. Soc. Rev.* **2001**, *30*, 113−124.

(8) Chen, L. X.; Shaw, G. B.; Novozhilova, I.; Liu, T.; Jennings, G.; Attenkofer, K.; Meyer, G. J.; Coppens, P. MLCT state structure and dynamics of a copper(I) diimine complex characterized by pump-probe X-ray and laser spectroscopies and DFT calculations. *J. Am. Chem. Soc.* **2003**, *125*, 7022−7034.

(9) Siddique, Z. A.; Yamamoto, Y.; Ohno, T.; Nozaki, K. Structure-dependent photophysical properties of singlet and triplet metal-to-ligand charge transfer states in copper(I) bis(diimine) compounds. *Inorg. Chem.* **2003**, *42*, 6366−6378.

(10) Hamze, R.; Peltier, J. L.; Sylvinson, D.; Jung, M.; Cardenas, J.; Haiges, R.; Soleilhavoup, M.; Jazzar, R.; Djurovich, P. I.; Bertrand, G.; Thompson, M. E. Eliminating nonradiative decay in Cu^{I} emitters: >99% quantum efficiency and microsecond lifetime. *Science* **2019**, *363*, 601−606.

(11) Di, D. W.; Romanov, A. S.; Yang, L.; Richter, J. M.; Rivett, J. P. H.; Jones, S.; Thomas, T. H.; Jalebi, M. A.; Friend, R. H.; Linnolahti, M.; Bochmann, M.; Credgington, D. High-performance light-emitting diodes based on carbene-metal-amides. *Science* **2017**, *356*, 159−163.

(12) Gernert, M.; Balles-Wolf, L.; Kerner, F.; Müller, U.; Schmiedel, A.; Holzapfel, M.; Marian, C. M.; Pflaum, J.; Lambert, C.; Steffen, A. Cyclic (Amino)(aryl)carbenes Enter the Field of Chromophore Ligands: Expanded π System Leads to Unusually Deep Red Emitting Cu^{I} Compounds. *J. Am. Chem. Soc.* **2020**, *142*, 8897−8909.

(13) Czerwieniec, R.; Leitl, M. J.; Homeier, H. H. H.; Yersin, H. Cu(I) Complexes - Thermally Activated Delayed Fluorescence. Photophysical Approach and Material Design. *Coord. Chem. Rev.* **2016**, *325*, 2−28.

(14) Housecroft, C. E.; Constable, E. C. Solar energy conversion using first row d-block metal coordination compound sensitizers and redox mediators. *Chem. Sci.* **2022**, *13*, 1225−1262.

(15) Eberhart, M. S.; Phelan, B. T.; Niklas, J.; Sprague-Klein, E. A.; Kaphan, D. M.; Gosztola, D. J.; Chen, L. X.; Tiede, D. M.; Poluektov, O. G.; Mulfort, K. L. Surface immobilized copper(I) diimine photosensitizers as molecular probes for elucidating the effects of confinement at interfaces for solar energy conversion. *Chem. Commun.* **2020**, *56*, 12130−12133.

(16) Hossain, A.; Bhattacharyya, A.; Reiser, O. Copper's rapid ascent in visible-light photoredox catalysis. *Science* **2019**, *364*, eaav9713.

(17) Reiser, O. Shining Light on Copper: Unique Opportunities for Visible-Light-Catalyzed Atom Transfer Radical Addition Reactions and Related Processes. *Acc. Chem. Res.* **2016**, *49*, 1990−1996.

(18) Hernandez-Perez, A. C.; Collins, S. K. Heteroleptic Cu-Based Sensitizers in Photoredox Catalysis. *Acc. Chem. Res.* **2016**, *49*, 1557−1565.

(19) Büldt, L. A.; Wenger, O. S. Chromium Complexes for Luminescence, Solar Cells, Photoredox Catalysis, Upconversion, and Phototriggered NO Release. *Chem. Sci.* **2017**, *8*, 7359−7367.

(20) Kitzmann, W. R.; Moll, J.; Heinze, K. Spin-flip luminescence. *Photochem. Photobiol. Sci.* **2022**, *21*, 1309−1331.

(21) Hauser, A.; Reber, C. Spectroscopy and Chemical Bonding in Transition Metal Complexes. In *Structure and Bonding*, 2017; Vol. *172*, pp 291−312.

(22) Otto, S.; Grabolle, M.; Förster, C.; Kreitner, C.; Resch-Genger, U.; Heinze, K. $Cr(ddpd)_2^{3+}$: A Molecular, Water-Soluble, Highly

NIR-Emissive Ruby Analogue. *Angew. Chem., Int. Ed.* **2015**, *54*, 11572−11576.
(23) Wang, C.; Otto, S.; Dorn, M.; Kreidt, E.; Lebon, J.; Sršan, L.; Di Martino-Fumo, P.; Gerhards, M.; Resch-Genger, U.; Seitz, M.; Heinze, K. Deuterated Molecular Ruby with Record Luminescence Quantum Yield. *Angew. Chem., Int. Ed.* **2018**, *57*, 1112−1116.
(24) Treiling, S.; Wang, C.; Förster, C.; Reichenauer, F.; Kalmbach, J.; Boden, P.; Harris, J.; Carrella, L.; Rentschler, E.; Resch-Genger, U.; Reber, C.; Seitz, M.; Gerhards, M.; Heinze, K. Luminescence and Light-Driven Energy and Electron Transfer from an Exceptionally Long-Lived Excited State of a Non-Innocent Chromium(III) Complex. *Angew. Chem., Int. Ed.* **2019**, *58*, 18075−18085.
(25) Reichenauer, F.; Wang, C.; Förster, C.; Boden, P.; Ugur, N.; Báez-Cruz, R.; Kalmbach, J.; Carrella, L.; Rentschler, E.; Ramanan, C.; Niedner-Schatteburg, G.; Gerhards, M.; Seitz, M.; Resch-Genger, U.; Heinze, K. Strongly Red-Emissive Molecular Ruby $[Cr(bpmp)_2]^{3+}$ surpasses $[Ru(bpy)_3]^{2+}$. *J. Am. Chem. Soc.* **2021**, *143*, 11843−11855.
(26) Jiménez, J.-R.; Poncet, M.; Míguez-Lago, S.; Grass, S.; Lacour, J.; Besnard, C.; Cuerva, J. M.; Campaña, A. G.; Piguet, C. Bright Long-Lived Circularly Polarized Luminescence in Chiral Chromium(III) Complexes. *Angew. Chem., Int. Ed.* **2021**, *60*, 10095−10102.
(27) Jiménez, J.-R.; Doistau, B.; Cruz, C. M.; Besnard, C.; Cuerva, J. M.; Campagña, A. G.; Piguet, C. Chiral Molecular Ruby $[Cr(dqp)_2]^{3+}$ with Long-Lived Circularly Polarized Luminescence. *J. Am. Chem. Soc.* **2019**, *141*, 13244−13252.
(28) Aboshyan-Sorgho, L.; Cantuel, M.; Petoud, S.; Hauser, A.; Piguet, C. Optical Sensitization and Upconversion in Discrete Polynuclear Chromium-Lanthanide Complexes. *Coord. Chem. Rev.* **2012**, *256*, 1644−1663.
(29) Sinha, N.; Jiménez, J. R.; Pfund, B.; Prescimone, A.; Piguet, C.; Wenger, O. S. A Near-Infrared-II Emissive Chromium(III) Complex. *Angew. Chem., Int. Ed.* **2021**, *60*, 23722−23728.
(30) Higgins, R. F.; Fatur, S. M.; Shepard, S. G.; Stevenson, S. M.; Boston, D. J.; Ferreira, E. M.; Damrauer, N. H.; Rappé, A. K.; Shores, M. P. Uncovering the Roles of Oxygen in Cr^{III} Photoredox Catalysis. *J. Am. Chem. Soc.* **2016**, *138*, 5451−5464.
(31) Stevenson, S. M.; Shores, M. P.; Ferreira, E. M. Photooxidizing Chromium Catalysts for Promoting Radical Cation Cycloadditions. *Angew. Chem., Int. Ed.* **2015**, *54*, 6506−6510.
(32) Soupart, A.; Alary, F.; Heully, J.-L.; Elliott, P. I. P.; Dixon, I. M. Recent progress in ligand photorelease reaction mechanisms: Theoretical insights focusing on Ru(II) ^{3}MC states. *Coord. Chem. Rev.* **2020**, *408*, 213184−213193.
(33) Juris, A.; Balzani, V.; Barigelletti, F.; Campagna, S.; Belser, P.; Von Zelewsky, A. Ru(II) Polypyridine Complexes - Photophysics, Photochemistry, Electrochemistry, and Chemiluminescence. *Coord. Chem. Rev.* **1988**, *84*, 85−277.
(34) Mills, I. N.; Porras, J. A.; Bernhard, S. Judicious Design of Cationic, Cyclometalated Ir^{III} Complexes for Photochemical Energy Conversion and Optoelectronics. *Acc. Chem. Res.* **2018**, *51*, 352−364.
(35) Shon, J. H.; Teets, T. S. Molecular Photosensitizers in Energy Research and Catalysis: Design Principles and Recent Developments. *ACS Energy Lett.* **2019**, *4*, 558−566.
(36) Bevernaegie, R.; Wehlin, S. A. M.; Elias, B.; Troian-Gautier, L. A Roadmap Towards Visible Light Mediated Electron Transfer Chemistry with Iridium(III) Complexes. *ChemPhotoChem* **2021**, *5*, 217−234.
(37) Bevernaegie, R.; Wehlin, S. A. M.; Piechota, E. J.; Abraham, M.; Philouze, C.; Meyer, G. J.; Elias, B.; Troian-Gautier, L. Improved Visible Light Absorption of Potent Iridium(III) Photo-oxidants for Excited-State Electron Transfer Chemistry. *J. Am. Chem. Soc.* **2020**, *142*, 2732−2737.
(38) Baldo, M. A.; O'Brien, D. F.; You, Y.; Shoustikov, A.; Sibley, S.; Thompson, M. E.; Forrest, S. R. Highly efficient phosphorescent emission from organic electroluminescent devices. *Nature* **1998**, *395*, 151−154.
(39) Brooks, J.; Babayan, Y.; Lamansky, S.; Djurovich, P. I.; Tsyba, I.; Bau, R.; Thompson, M. E. Synthesis and characterization of phosphorescent cyclometalated platinum complexes. *Inorg. Chem.* **2002**, *41*, 3055−3066.
(40) Suzuki, S.; Sugimura, R.; Kozaki, M.; Keyaki, K.; Nozaki, K.; Ikeda, N.; Akiyama, K.; Okada, K. Highly efficient photoproduction of charge-separated states in donor-acceptor-linked bis(acetylide) platinum complexes. *J. Am. Chem. Soc.* **2009**, *131*, 10374−10375.
(41) Strassert, C. A.; Chien, C. H.; Galvez Lopez, M. D.; Kourkoulos, D.; Hertel, D.; Meerholz, K.; De Cola, L. Switching on luminescence by the self-assembly of a platinum(II) complex into gelating nanofibers and electroluminescent films. *Angew. Chem., Int. Ed.* **2011**, *50*, 946−950.
(42) Kalinowski, J.; Fattori, V.; Cocchi, M.; Williams, J. A. G. Light-emitting devices based on organometallic platinum complexes as emitters. *Coord. Chem. Rev.* **2011**, *255*, 2401−2425.
(43) Yam, V. W.; Au, V. K.; Leung, S. Y. Light-Emitting Self-Assembled Materials Based on d^8 and d^{10} Transition Metal Complexes. *Chem. Rev.* **2015**, *115*, 7589−7728.
(44) Aliprandi, A.; Mauro, M.; De Cola, L. Controlling and imaging biomimetic self-assembly. *Nat. Chem.* **2016**, *8*, 10−15.
(45) Saito, D.; Ogawa, T.; Yoshida, M.; Takayama, J.; Hiura, S.; Murayama, A.; Kobayashi, A.; Kato, M. Intense Red-Blue Luminescence Based on Superfine Control of Metal-Metal Interactions for Self-Assembled Platinum(II) Complexes. *Angew. Chem., Int. Ed.* **2020**, *59*, 18723−18730.
(46) Deaton, J. C.; Chakraborty, A.; Czerwieniec, R.; Yersin, H.; Castellano, F. N. Temperature dependence of photophysical properties of a dinuclear C∧N-cyclometalated Pt(II) complex with an intimate Pt-Pt contact. Zero-field splitting and sub-state decay rates of the lowest triplet. *Phys. Chem. Chem. Phys.* **2018**, *20*, 25096−25104.
(47) Straub, L.; González-Abradelo, D.; Strassert, C. A. Oxygen-insensitive phosphorescence in water from a Pt-doped supramolecular array. *Chem. Commun.* **2017**, *53*, 11806−11809.
(48) Horiuchi, S.; Moon, S.; Ito, A.; Tessarolo, J.; Sakuda, E.; Arikawa, Y.; Clever, G. H.; Umakoshi, K. Multinuclear Ag Clusters Sandwiched by Pt Complex Units: Fluxional Behavior and Chiral-at-Cluster Photoluminescence. *Angew. Chem., Int. Ed.* **2021**, *60*, 10654−10660.
(49) Horiuchi, S.; Hiroiwa, H.; Sakuda, E.; Arikawa, Y.; Umakoshi, K. An asymmetric Pt diimine acetylide complex providing unique luminescent multinuclear sandwich complexes with Cu salts. *Chem. Commun.* **2022**, *58*, 3489−3492.
(50) Malmberg, R.; Venkatesan, K. Conceptual advances in the preparation and excited-state properties of neutral luminescent (C∧N) and (C∧C*) monocyclometalated gold(III) complexes. *Coord. Chem. Rev.* **2021**, *449*, 214182−214203.
(51) Tang, M. C.; Chan, M. Y.; Yam, V. W. Molecular Design of Luminescent Gold(III) Emitters as Thermally Evaporable and Solution-Processable Organic Light-Emitting Device (OLED) Materials. *Chem. Rev.* **2021**, *121*, 7249−7279.
(52) Carey, M. C.; Adelman, S. L.; McCusker, J. K. Insights into the excited state dynamics of Fe(II) polypyridyl complexes from variable-temperature ultrafast spectroscopy. *Chem. Sci.* **2019**, *10*, 134−144.
(53) McCusker, J. K.; Walda, K. N.; Dunn, R. C.; Simon, J. D.; Magde, D.; Hendrickson, D. N. Subpicosecond ^{1}MLCT-$^5T_2$ Intersystem Crossing of Low-Spin Polypyridyl Ferrous Complexes. *J. Am. Chem. Soc.* **1993**, *115*, 298−307.
(54) Paulus, B. C.; Adelman, S. L.; Jamula, L. L.; McCusker, J. K. Leveraging excited-state coherence for synthetic control of ultrafast dynamics. *Nature* **2020**, *582*, 214−218.
(55) Zhang, W.; Gaffney, K. J. Mechanistic Studies of Photoinduced Spin Crossover and Electron Transfer in Inorganic Complexes. *Acc. Chem. Res.* **2015**, *48*, 1140−1148.
(56) Tatsuno, H.; Kjær, K. S.; Kunnus, K.; Harlang, T. C. B.; Timm, C.; Guo, M.; Chàbera, P.; Fredin, L. A.; Hartsock, R. W.; Reinhard, M. E.; Koroidov, S.; Li, L.; Cordones, A. A.; Gordivska, O.; Prakash, O.; Liu, Y.; Laursen, M. G.; Biasin, E.; Hansen, F. B.; Vester, P.; Christensen, M.; Haldrup, K.; Németh, Z.; Sárosiné Szemes, D.; Bajnóczi, É.; Vankó, G.; Van Driel, T. B.; Alonso-Mori, R.; Glownia, J. M.; Nelson, S.; Sikorski, M.; Lemke, H. T.; Sokaras, D.; Canton, S. E.;

Dohn, A. O.; Møller, K. B.; Nielsen, M. M.; Gaffney, K. J.; Wärnmark, K.; Sundström, V.; Persson, P.; Uhlig, J. Hot Branching Dynamics in a Light-Harvesting Iron Carbene Complex Revealed by Ultrafast X-ray Emission Spectroscopy. *Angew. Chem., Int. Ed.* **2020**, *59*, 364−372.
(57) Kjær, K. S.; Van Driel, T. B.; Harlang, T. C. B.; Kunnus, K.; Biasin, E.; Ledbetter, K.; Hartsock, R. W.; Reinhard, M. E.; Koroidov, S.; Li, L.; Laursen, M. G.; Hansen, F. B.; Vester, P.; Christensen, M.; Haldrup, K.; Nielsen, M. M.; Dohn, A. O.; Pápai, M. I.; Møller, K. B.; Chabera, P.; Liu, Y.; Tatsuno, H.; Timm, C.; Jarenmark, M.; Uhlig, J.; Sundström, V.; Wärnmark, K.; Persson, P.; Németh, Z.; Szemes, D. S.; Bajnóczi, É.; Vankó, G.; Alonso-Mori, R.; Glownia, J. M.; Nelson, S.; Sikorski, M.; Sokaras, D.; Canton, S. E.; Lemke, H. T.; Gaffney, K. J. Finding intersections between electronic excited state potential energy surfaces with simultaneous ultrafast X-ray scattering and spectroscopy. *Chem. Sci.* **2019**, *10*, 5749−5760.
(58) Dierks, P.; Vukadinovic, Y.; Bauer, M. Photoactive iron complexes: more sustainable, but still a challenge. *Inorg. Chem. Front.* **2022**, *9*, 206−220.
(59) Reuter, T.; Kruse, A.; Schoch, R.; Lochbrunner, S.; Bauer, M.; Heinze, K. Higher MLCT lifetime of carbene iron(II) complexes by chelate ring expansion. *Chem. Commun.* **2021**, *57*, 7541−7544.
(60) Liu, Y.; Harlang, T.; Canton, S. E.; Chábera, P.; Suárez-Alcántara, K.; Fleckhaus, A.; Vithanage, D. A.; Göransson, E.; Corani, A.; Lomoth, R.; Sundström, V.; Wärnmark, K. Towards Longer-Lived Metal-to-Ligand Charge Transfer States of Iron(II) Complexes: An N-Heterocyclic Carbene Approach. *Chem. Commun.* **2013**, *49*, 6412−6414.
(61) Harlang, T. C. B.; Liu, Y. Z.; Gordivska, O.; Fredin, L. A.; Ponseca, C. S.; Huang, P.; Chabera, P.; Kjaer, K. S.; Mateos, H.; Uhlig, J.; Lomoth, R.; Wallenberg, R.; Styring, S.; Persson, P.; Sundström, V.; Wärnmark, K. Iron Sensitizer Converts Light to Electrons with 92% Yield. *Nat. Chem.* **2015**, *7*, 883−889.
(62) Liu, Y.; Persson, P.; Sundström, V.; Wärnmark, K. Fe N-heterocyclic carbene complexes as promising photosensitizers. *Acc. Chem. Res.* **2016**, *49*, 1477−1485.
(63) Chábera, P.; Kjaer, K. S.; Prakash, O.; Honarfar, A.; Liu, Y.; Fredin, L. A.; Harlang, T. C. B.; Lidin, S.; Uhlig, J.; Sundström, V.; Lomoth, R.; Persson, P.; Wärnmark, K. Fe^{II} hexa N-heterocyclic carbene complex with a 528 ps metal-to-ligand charge-transfer excited-state lifetime. *J. Phys. Chem. Lett.* **2018**, *9*, 459−463.
(64) Cebrián, C.; Pastore, M.; Monari, A.; Assfeld, X.; Gros, P. C.; Haacke, S. Ultrafast Spectroscopy of Fe(II) Complexes Designed for Solar Energy Conversion: Current Status and Open Questions. *ChemPhysChem* **2022**, *23*, e202100659.
(65) Liu, L.; Duchanois, T.; Etienne, T.; Monari, A.; Beley, M.; Assfeld, X.; Haacke, S.; Gros, P. C. A New Record Excited State ^{3}MLCT Lifetime for Metalorganic Iron(II) Complexes. *Phys. Chem. Chem. Phys.* **2016**, *18*, 12550−12556.
(66) Francés-Monerris, A.; Magra, K.; Darari, M.; Cebrián, C.; Beley, M.; Domenichini, E.; Haacke, S.; Pastore, M.; Assfeld, X.; Gros, P. C.; Monari, A. Synthesis and Computational Study of a Pyridylcarbene Fe(II) Complex: Unexpected Effects of fac/mer Isomerism in Metal-to-Ligand Triplet Potential Energy Surfaces. *Inorg. Chem.* **2018**, *57*, 10431−10441.
(67) Braun, J. D.; Lozada, I. B.; Kolodziej, C.; Burda, C.; Newman, K. M. E.; van Lierop, J.; Davis, R. L.; Herbert, D. E. Iron(II) coordination complexes with panchromatic absorption and nanosecond charge-transfer excited state lifetimes. *Nat. Chem.* **2019**, *11*, 1144−1150.
(68) Sinha, N.; Pfund, B.; Wegeberg, C.; Prescimone, A.; Wenger, O. S. Cobalt(III) Carbene Complex with an Electronic Excited-State Structure Similar to Cyclometalated Iridium(III) Compounds. *J. Am. Chem. Soc.* **2022**, *144*, 9859−9873.
(69) Herr, P.; Kerzig, C.; Larsen, C. B.; Häussinger, D.; Wenger, O. S. Manganese(I) complexes with metal-to-ligand charge transfer luminescence and photoreactivity. *Nat. Chem.* **2021**, *13*, 956−962.
(70) Büldt, L. A.; Guo, X.; Vogel, R.; Prescimone, A.; Wenger, O. S. A tris(diisocyanide)chromium(0) complex is a luminescent analog of $Fe(2,2'\text{-bipyridine})_3^{2+}$. *J. Am. Chem. Soc.* **2017**, *139*, 985−992.
(71) Wegeberg, C.; Häussinger, D.; Wenger, O. S. Pyrene-Decoration of a Chromium(0) Tris(diisocyanide) Enhances Excited State Delocalization: A Strategy to Improve the Photoluminescence of $3d^6$ Metal Complexes. *J. Am. Chem. Soc.* **2021**, *143*, 15800−15811.
(72) Wegeberg, C.; Wenger, O. S. Luminescent chromium(0) and manganese(I) complexes. *Dalton Trans.* **2022**, *51*, 1297−1302.
(73) Bussière, G.; Reber, C. Coupled excited states in nickel(II) complexes probed by polarized absorption spectroscopy. *J. Am. Chem. Soc.* **1998**, *120*, 6306−6315.
(74) Oppenheim, J. J.; McNicholas, B. J.; Miller, J.; Gray, H. B. Electronic Structure of Tetracyanonickelate(II). *Inorg. Chem.* **2019**, *58*, 15202−15206.
(75) Wenger, O. S. Vapochromism in organometallic and coordination complexes: chemical sensors for volatile organic compounds. *Chem. Rev.* **2013**, *113*, 3686−3733.
(76) Iwamura, M.; Fukui, A.; Nozaki, K.; Kuramochi, H.; Takeuchi, S.; Tahara, T. Coherent Vibration and Femtosecond Dynamics of the Platinum Complex Oligomers upon Intermolecular Bond Formation in the Excited State. *Angew. Chem., Int. Ed.* **2020**, *59*, 23154−23161.
(77) Wong, Y. S.; Tang, M. C.; Ng, M.; Yam, V. W. Toward the Design of Phosphorescent Emitters of Cyclometalated Earth-Abundant Nickel(II) and Their Supramolecular Study. *J. Am. Chem. Soc.* **2020**, *142*, 7638−7646.
(78) Andrews, L. J. Radiationless decay in rhodium(I) and iridium(I) complexes. Polarization and solvent relaxation studies. *J. Phys. Chem.* **1979**, *83*, 3203−3209.
(79) Kurz, H.; Schötz, K.; Papadopoulos, I.; Heinemann, F. W.; Maid, H.; Guldi, D. M.; Köhler, A.; Hörner, G.; Weber, B. A Fluorescence-Detected Coordination-Induced Spin State Switch. *J. Am. Chem. Soc.* **2021**, *143*, 3466−3480.
(80) Cope, J. D.; Denny, J. A.; Lamb, R. W.; McNamara, L. E.; Hammer, N. I.; Webster, C. E.; Hollis, T. K. Synthesis, characterization, photophysics, and a ligand rearrangement of CCC-NHC pincer nickel complexes: Colors, polymorphs, emission, and Raman spectra. *J. Organomet. Chem.* **2017**, *845*, 258−265.
(81) Ryland, E. S.; Zhang, K.; Vura-Weis, J. Sub-100 fs Intersystem Crossing to a Metal-Centered Triplet in Ni(II)OEP Observed with M-Edge XANES. *J. Phys. Chem. A* **2019**, *123*, 5214−5222.
(82) Phelan, B. T.; Mara, M. W.; Chen, L. X. Excited-state structural dynamics of nickel complexes probed by optical and X-ray transient absorption spectroscopies: insights and implications. *Chem. Commun.* **2021**, *57*, 11904−11921.
(83) Plyusnin, V. F.; Pozdnyakov, I. P.; Grivin, V. P.; Solovyev, A. I.; Lemmetyinen, H.; Tkachenko, N. V.; Larionov, S. V. Femtosecond spectroscopy of the dithiolate Cu(II) and Ni(II) complexes. *Dalton Trans.* **2014**, *43*, 17766−17774.
(84) Frei, F.; Rondi, A.; Espa, D.; Mercuri, M. L.; Pilia, L.; Serpe, A.; Odeh, A.; Van Mourik, F.; Chergui, M.; Feurer, T.; Deplano, P.; Vlček, A.; Cannizzo, A. Ultrafast electronic and vibrational relaxations in mixed-ligand dithione-dithiolato Ni, Pd, and Pt complexes. *Dalton Trans.* **2014**, *43*, 17666−17676.
(85) Dorn, M.; Mack, K.; Carrella, L. M.; Rentschler, E.; Förster, C.; Heinze, K. Structure and Electronic Properties of an Expanded Terpyridine Complex of Nickel(II) $[Ni(ddpd)_2](BF_4)_2$. *Z. Anorg. Allg. Chem.* **2018**, *644*, 706−712.
(86) Wojnar, M. K.; Laorenza, D. W.; Schaller, R. D.; Freedman, D. E. Nickel(II) Metal Complexes as Optically Addressable Qubit Candidates. *J. Am. Chem. Soc.* **2020**, *142*, 14826−14830.
(87) Zuo, Z.; Ahneman, D. T.; Chu, L.; Terrett, J. A.; Doyle, A. G.; MacMillan, D. W. Dual catalysis. Merging photoredox with nickel catalysis: coupling of alpha-carboxyl sp^3-carbons with aryl halides. *Science* **2014**, *345*, 437−440.
(88) Terrett, J. A.; Cuthbertson, J. D.; Shurtleff, V. W.; MacMillan, D. W. Switching on elusive organometallic mechanisms with photoredox catalysis. *Nature* **2015**, *524*, 330−334.
(89) Heitz, D. R.; Tellis, J. C.; Molander, G. A. Photochemical Nickel-Catalyzed C-H Arylation: Synthetic Scope and Mechanistic Investigations. *J. Am. Chem. Soc.* **2016**, *138*, 12715−12718.

https://doi.org/10.1021/jacs.2c08838
J. Am. Chem. Soc. 2022, 144, 21948−21960

(90) Ahneman, D. T.; Doyle, A. G. C-H functionalization of amines with aryl halides by nickel-photoredox catalysis. *Chem. Sci.* **2016**, *7*, 7002−7006.
(91) Shields, B. J.; Doyle, A. G. Direct C(sp^3)-H Cross Coupling Enabled by Catalytic Generation of Chlorine Radicals. *J. Am. Chem. Soc.* **2016**, *138*, 12719−12722.
(92) Welin, E. R.; Le, C.; Arias-Rotondo, D. M.; McCusker, J. K.; MacMillan, D. W. Photosensitized, energy transfer-mediated organometallic catalysis through electronically excited nickel(II). *Science* **2017**, *355*, 380−385.
(93) Shields, B. J.; Kudisch, B.; Scholes, G. D.; Doyle, A. G. Long-Lived Charge-Transfer States of Nickel(II) Aryl Halide Complexes Facilitate Bimolecular Photoinduced Electron Transfer. *J. Am. Chem. Soc.* **2018**, *140*, 3035−3039.
(94) Lim, C. H.; Kudisch, M.; Liu, B.; Miyake, G. M. C-N Cross-Coupling via Photoexcitation of Nickel-Amine Complexes. *J. Am. Chem. Soc.* **2018**, *140*, 7667−7673.
(95) Tian, L.; Till, N. A.; Kudisch, B.; MacMillan, D. W. C.; Scholes, G. D. Transient Absorption Spectroscopy Offers Mechanistic Insights for an Iridium/Nickel-Catalyzed C-O Coupling. *J. Am. Chem. Soc.* **2020**, *142*, 4555−4559.
(96) Ting, S. I.; Garakyaraghi, S.; Taliaferro, C. M.; Shields, B. J.; Scholes, G. D.; Castellano, F. N.; Doyle, A. G. ^{3}d-d Excited States of Ni(II) Complexes Relevant to Photoredox Catalysis: Spectroscopic Identification and Mechanistic Implications. *J. Am. Chem. Soc.* **2020**, *142*, 5800−5810.
(97) Campbell, M. W.; Yuan, M.; Polites, V. C.; Gutierrez, O.; Molander, G. A. Photochemical C-H Activation Enables Nickel-Catalyzed Olefin Dicarbofunctionalization. *J. Am. Chem. Soc.* **2021**, *143*, 3901−3910.
(98) Tasker, S. Z.; Standley, E. A.; Jamison, T. F. Recent advances in homogeneous nickel catalysis. *Nature* **2014**, *509*, 299−309.
(99) Hazari, N.; Melvin, P. R.; Beromi, M. M. Well-defined nickel and palladium precatalysts for cross-coupling. *Nat. Rev. Chem.* **2017**, *1*, 0025.
(100) Kudisch, M.; Lim, C. H.; Thordarson, P.; Miyake, G. M. Energy Transfer to Ni-Amine Complexes in Dual Catalytic, Light-Driven C-N Cross-Coupling Reactions. *J. Am. Chem. Soc.* **2019**, *141*, 19479−19486.
(101) Na, H.; Mirica, L. M. Deciphering the mechanism of the Ni-photocatalyzed C−O cross-coupling reaction using a tridentate pyridinophane ligand. *Nat. Commun.* **2022**, *13*, No. 1313.
(102) Cagan, D. A.; Stroscio, G. D.; Cusumano, A. Q.; Hadt, R. G. Multireference Description of Nickel-Aryl Homolytic Bond Dissociation Processes in Photoredox Catalysis. *J. Phys. Chem. A* **2020**, *124*, 9915−9922.
(103) Stratakes, B. M.; Wells, K. A.; Kurtz, D. A.; Castellano, F. N.; Miller, A. J. M. Photochemical H_2 Evolution from Bis(diphosphine)-nickel Hydrides Enables Low-Overpotential Electrocatalysis. *J. Am. Chem. Soc.* **2021**, *143*, 21388−21401.
(104) Cagan, D. A.; Bím, D.; Silva, B.; Kazmierczak, N. P.; McNicholas, B. J.; Hadt, R. G. Elucidating the Mechanism of Excited-State Bond Homolysis in Nickel-Bipyridine Photoredox Catalysts. *J. Am. Chem. Soc.* **2022**, *144*, 6516−6531.
(105) Williams, J. A. G.; Beeby, A.; Davies, E. S.; Weinstein, J. A.; Wilson, C. An alternative route to highly luminescent platinum(II) complexes: cyclometalation with N^C^N-coordinating dipyridylbenzene ligands. *Inorg. Chem.* **2003**, *42*, 8609−8611.
(106) Farley, S. J.; Rochester, D. L.; Thompson, A. L.; Howard, J. A.; Williams, J. A. G. Controlling emission energy, self-quenching, and excimer formation in highly luminescent N∧C∧N-coordinated platinum(II) complexes. *Inorg. Chem.* **2005**, *44*, 9690−9703.
(107) Tong, G.-M.; Che, C. M. Emissive or nonemissive? A theoretical analysis of the phosphorescence efficiencies of cyclometalated platinum(II) complexes. *Chem.−Eur. J.* **2009**, *15*, 7225−7237.
(108) Rausch, A. F.; Murphy, L.; Williams, J. A. G.; Yersin, H. Improving the performance of Pt(II) complexes for blue light emission by enhancing the molecular rigidity. *Inorg. Chem.* **2012**, *51*, 312−319.
(109) Prokhorov, A. M.; Hofbeck, T.; Czerwieniec, R.; Suleymanova, A. F.; Kozhevnikov, D. N.; Yersin, H. Brightly luminescent Pt(II) pincer complexes with a sterically demanding carboranyl-phenylpyridine ligand: a new material class for diverse optoelectronic applications. *J. Am. Chem. Soc.* **2014**, *136*, 9637−9642.
(110) Lin, W. J.; Naziruddin, A. R.; Chen, Y. H.; Sun, B. J.; Chang, A. H.; Wang, W. J.; Hwang, W. S. Photofunctional platinum complexes featuring N-heterocyclic carbene-based pincer ligands. *Chem. Asian J.* **2015**, *10*, 728−739.
(111) Cope, J. D.; Liyanage, N. P.; Kelley, P. J.; Denny, J. A.; Valente, E. J.; Webster, C. E.; Delcamp, J. H.; Hollis, T. K. Electrocatalytic reduction of CO_2 with CCC-NHC pincer nickel complexes. *Chem. Commun.* **2017**, *53*, 9442−9445.
(112) Danopoulos, A. A.; Simler, T.; Braunstein, P. N-Heterocyclic Carbene Complexes of Copper, Nickel, and Cobalt. *Chem. Rev.* **2019**, *119*, 3730−3961.
(113) Fox, B. J.; Millard, M. D.; DiPasquale, A. G.; Rheingold, A. L.; Figueroa, J. S. Thallium(I) as a coordination site protection agent: preparation of an isolable zero-valent nickel tris-isocyanide. *Angew. Chem., Int. Ed.* **2009**, *48*, 3473−3477.
(114) Carpenter, A. E.; McNeece, A. J.; Barnett, B. R.; Estrada, A. L.; Mokhtarzadeh, C. C.; Moore, C. E.; Rheingold, A. L.; Perrin, C. L.; Figueroa, J. S. Direct observation of beta-chloride elimination from an isolable beta-chloroalkyl complex of square-planar nickel. *J. Am. Chem. Soc.* **2014**, *136*, 15481−15484.
(115) Carpenter, A. E.; Mokhtarzadeh, C. C.; Ripatti, D. S.; Havrylyuk, I.; Kamezawa, R.; Moore, C. E.; Rheingold, A. L.; Figueroa, J. S. Comparative measure of the electronic influence of highly substituted aryl isocyanides. *Inorg. Chem.* **2015**, *54*, 2936−2944.
(116) Drance, M. J.; Sears, J. D.; Mrse, A. M.; Moore, C. E.; Rheingold, A. L.; Neidig, M. L.; Figueroa, J. S. Terminal coordination of diatomic boron monofluoride to iron. *Science* **2019**, *363*, 1203−1205.
(117) Mokhtarzadeh, C. C.; Chan, C.; Moore, C. E.; Rheingold, A. L.; Figueroa, J. S. Side-On Coordination of Nitrous Oxide to a Mononuclear Cobalt Center. *J. Am. Chem. Soc.* **2019**, *141*, 15003−15007.
(118) Ito, H.; Kato, T.; Sawamura, M. Design and synthesis of isocyanide ligands for catalysis: application to Rh-catalyzed hydrosilylation of ketones. *Chem. Asian J.* **2007**, *2*, 1436−1446.
(119) Monat, J. E.; McCusker, J. K. Femtosecond excited-state dynamics of an iron(II) polypyridyl solar cell sensitizer model. *J. Am. Chem. Soc.* **2000**, *122*, 4092−4097.
(120) Liu, Y.; Persson, P.; Sundström, V.; Wärnmark, K. Fe N-Heterocyclic Carbene Complexes as Promising Photosensitizers. *Acc. Chem. Res.* **2016**, *49*, 1477−1485.
(121) Chábera, P.; Liu, Y.; Prakash, O.; Thyrhaug, E.; Nahhas, A. E.; Honarfar, A.; Essén, S.; Fredin, L. A.; Harlang, T. C.; Kjær, K. S.; Handrup, K.; Ericson, F.; Tatsuno, H.; Morgan, K.; Schnadt, J.; Häggström, L.; Ericsson, T.; Sobkowiak, A.; Lidin, S.; Huang, P.; Styring, S.; Uhlig, J.; Bendix, J.; Lomoth, R.; Sundström, V.; Persson, P.; Wärnmark, K. A low-spin Fe(III) complex with 100-ps ligand-to-metal charge transfer photoluminescence. *Nature* **2017**, *543*, 695−699.
(122) Tanabiki, M.; Tsuchiya, K.; Kumanomido, Y.; Matsubara, K.; Motoyama, Y.; Nagashima, H. Nickel(II) Isocyanide Complexes as Ethylene Polymerization Catalysts. *Organometallics* **2004**, *23*, 3976−3981.
(123) Noda, D.; Tanabiki, M.; Tsuchiya, K.; Sunada, Y.; Nagashima, H. Mono- and bimetallic ethylene polymerization catalysts having an azanickellacyclopentene skeleton. *Polyhedron* **2009**, *28*, 3935−3944.
(124) Eskelinen, T.; Buss, S.; Petrovskii, S. K.; Grachova, E. V.; Krause, M.; Kletsch, L.; Klein, A.; Strassert, C. A.; Koshevoy, I. O.; Hirva, P. Photophysics and Excited State Dynamics of Cyclometalated [M(Phbpy)(CN)] (M = Ni, Pd, Pt) Complexes: A Theoretical and Experimental Study. *Inorg. Chem.* **2021**, *60*, 8777−8789.

https://doi.org/10.1021/jacs.2c08838
J. Am. Chem. Soc. 2022, 144, 21948−21960

(125) Deaton, J. C.; Taliaferro, C. M.; Pitman, C. L.; Czerwieniec, R.; Jakubikova, E.; Miller, A. J. M.; Castellano, F. N. Excited-State Switching between Ligand-Centered and Charge Transfer Modulated by Metal-Carbon Bonds in Cyclopentadienyl Iridium Complexes. *Inorg. Chem.* **2018**, *57*, 15445−15461.
(126) Yao, Y.; Ran, G.; Hou, C. L.; Zhang, R.; Mangel, D. N.; Yang, Z. S.; Zhu, M.; Zhang, W.; Zhang, J.; Sessler, J. L.; Gao, S.; Zhang, J. L. Nonaromatic Organonickel(II) Phototheranostics. *J. Am. Chem. Soc.* **2022**, *144*, 7346−7356.
(127) Shin, J.; Lee, J.; Suh, J. M.; Park, K. Ligand-field transition-induced C-S bond formation from nickelacycles. *Chem. Sci.* **2021**, *12*, 15908−15915.
(128) Grübel, M.; Bosque, I.; Altmann, P. J.; Bach, T.; Hess, C. R. Redox and photocatalytic properties of a Ni(II) complex with a macrocyclic biquinazoline (Mabiq) ligand. *Chem. Sci.* **2018**, *9*, 3313−3317.
(129) Lauenstein, R.; Mader, S. L.; Derondeau, H.; Esezobor, O. Z.; Block, M.; Römer, A. J.; Jandl, C.; Riedle, E.; Kaila, V. R. I.; Hauer, J.; Thyrhaug, E.; Hess, C. R. The central role of the metal ion for photoactivity: Zn- vs. Ni-Mabiq. *Chem. Sci.* **2021**, *12*, 7521−7532.
(130) Woodhouse, M. D.; McCusker, J. K. Mechanistic Origin of Photoredox Catalysis Involving Iron(II) Polypyridyl Chromophores. *J. Am. Chem. Soc.* **2020**, *142*, 16229−16233.
(131) Chung, L. H.; Chan, S. C.; Lee, W. C.; Wong, C. Y. Emissive osmium(II) complexes supported by N-heterocyclic carbene-based C∧C∧C-pincer ligands and aromatic diimines. *Inorg. Chem.* **2012**, *51*, 8693−8703.
(132) Creutz, C.; Chou, M.; Netzel, T. L.; Okumura, M.; Sutin, N. Lifetimes, spectra, and quenching of the excited states of polypyridine complexes of iron(II), ruthenium(II), and osmium(II). *J. Am. Chem. Soc.* **1980**, *102*, 1309−1319.
(133) Auböck, G.; Chergui, M. Sub-50-fs photoinduced spin crossover in $[Fe(bpy)_3]^{2+}$. *Nat. Chem.* **2015**, *7*, 629−633.
(134) Smeigh, A. L.; Creelman, M.; Mathies, R. A.; McCusker, J. K. Femtosecond time-resolved optical and Raman spectroscopy of photoinduced spin crossover: temporal resolution of low-to-high spin optical switching. *J. Am. Chem. Soc.* **2008**, *130*, 14105−14107.
(135) Oppermann, M.; Zinna, F.; Lacour, J.; Chergui, M. Chiral control of spin-crossover dynamics in Fe(II) complexes. *Nat. Chem.* **2022**, *14*, 739−745.
(136) Chen, L. X.; Shelby, M. L.; Lestrange, P. J.; Jackson, N. E.; Haldrup, K.; Mara, M. W.; Stickrath, A. B.; Zhu, D.; Lemke, H.; Chollet, M.; Hoffman, B. M.; Li, X. Imaging ultrafast excited state pathways in transition metal complexes by X-ray transient absorption and scattering using X-ray free electron laser source. *Faraday Discuss.* **2016**, *194*, 639−658.
(137) Chergui, M. Ultrafast photophysics of transition metal complexes. *Acc. Chem. Res.* **2015**, *48*, 801−808.
(138) Gawelda, W.; Cannizzo, A.; Pham, V. T.; van Mourik, F.; Bressler, C.; Chergui, M. Ultrafast nonadiabatic dynamics of $[Fe(II)(bpy)_3]^{2+}$ in solution. *J. Am. Chem. Soc.* **2007**, *129*, 8199−8206.
(139) Shelby, M. L.; Lestrange, P. J.; Jackson, N. E.; Haldrup, K.; Mara, M. W.; Stickrath, A. B.; Zhu, D.; Lemke, H. T.; Chollet, M.; Hoffman, B. M.; Li, X.; Chen, L. X. Ultrafast Excited State Relaxation of a Metalloporphyrin Revealed by Femtosecond X-ray Absorption Spectroscopy. *J. Am. Chem. Soc.* **2016**, *138*, 8752−8764.
(140) Lu, W.; Mi, B. X.; Chan, M. C.; Hui, Z.; Che, C. M.; Zhu, N.; Lee, S. T. Light-emitting tridentate cyclometalated platinum(II) complexes containing σ-alkynyl auxiliaries: tuning of photo- and electrophosphorescence. *J. Am. Chem. Soc.* **2004**, *126*, 4958−4971.
(141) Hissler, M.; McGarrah, J. E.; Connick, W. B.; Geiger, D. K.; Cummings, S. D.; Eisenberg, R. Platinum diimine complexes: towards a molecular photochemical device. *Coord. Chem. Rev.* **2000**, *208*, 115−137.
(142) Whittle, C. E.; Weinstein, J. A.; George, M. W.; Schanze, K. S. Photophysics of diimine platinum(II) bis-acetylide complexes. *Inorg. Chem.* **2001**, *40*, 4053−4062.
(143) Ogawa, T.; Sameera, W. M. C.; Yoshida, M.; Kobayashi, A.; Kato, M. Phosphorescence properties of anionic cyclometalated platinum(II) complexes with fluorine-substituted tridentate diphenylpyridine in the solid state. *Chem. Phys. Lett.* **2020**, *739*, 137024−137029.
(144) Ghosh, I.; Ghosh, T.; Bardagi, J. I.; König, B. Reduction of aryl halides by consecutive visible light-induced electron transfer processes. *Science* **2014**, *346*, 725−728.
(145) Haimerl, J.; Ghosh, I.; König, B.; Vogelsang, J.; Lupton, J. M. Single-molecule photoredox catalysis. *Chem. Sci.* **2019**, *10*, 681−687.
(146) Zeman, C. J. t.; Kim, S.; Zhang, F.; Schanze, K. S. Direct Observation of the Reduction of Aryl Halides by a Photoexcited Perylene Diimide Radical Anion. *J. Am. Chem. Soc.* **2020**, *142*, 2204−2207.
(147) MacKenzie, I. A.; Wang, L.; Onuska, N. P. R.; Williams, O. F.; Begam, K.; Moran, A. M.; Dunietz, B. D.; Nicewicz, D. A. Discovery and characterization of an acridine radical photoreductant. *Nature* **2020**, *580*, 76−80.
(148) Rieth, A. J.; Gonzalez, M. I.; Kudisch, B.; Nava, M.; Nocera, D. G. How Radical Are "Radical" Photocatalysts? A Closed-Shell Meisenheimer Complex Is Identified as a Super-Reducing Photoreagent. *J. Am. Chem. Soc.* **2021**, *143*, 14352−14359.
(149) Glaser, F.; Wenger, O. S. Red Light-Based Dual Photoredox Strategy Resembling the Z-Scheme of Natural Photosynthesis. *JACS Au* **2022**, *2*, 1488−1503.
(150) Na, H.; Maity, A.; Teets, T. S. Postsynthetic Systematic Electronic Tuning of Organoplatinum Photosensitizers via Secondary Coordination Sphere Interactions. *Organometallics* **2016**, *35*, 2267−2274.
(151) Schmid, L.; Glaser, F.; Schaer, R.; Wenger, O. S. High Triplet Energy Iridium(III) Isocyanoborato Complex for Photochemical Upconversion, Photoredox and Energy Transfer Catalysis. *J. Am. Chem. Soc.* **2022**, *144*, 963−976.
(152) Derrick, J. S.; Loipersberger, M.; Nistanaki, S. K.; Rothweiler, A. V.; Head-Gordon, M.; Nichols, E. M.; Chang, C. J. Templating Bicarbonate in the Second Coordination Sphere Enhances Electrochemical CO_2 Reduction Catalyzed by Iron Porphyrins. *J. Am. Chem. Soc.* **2022**, *144*, 11656−11663.
(153) Drover, M. W. A guide to secondary coordination sphere editing. *Chem. Soc. Rev.* **2022**, *51*, 1861−1880.

https://doi.org/10.1021/jacs.2c08838
J. Am. Chem. Soc. 2022, 144, 21948−21960